

Structural and functional brain changes in delusional disorder

Victor Vicens, Joaquim Radua, Raymond Salvador, Maria Anguera-Camós, Erick J. Canales-Rodríguez, Salvador Sarró, Teresa Maristany, Peter J. McKenna* and Edith Pomarol-Clotet*

Background

Delusional disorder has been the subject of very little investigation using brain imaging.

Aims

To examine potential structural and/or functional brain abnormalities in this disorder.

Method

We used structural imaging (voxel-based morphometry, VBM) and functional imaging (during performance of the *n*-back task and whole-brain resting connectivity analysis) to examine 22 patients meeting DSM-IV criteria for delusional disorder and 44 matched healthy controls.

Results

The patients showed grey matter reductions in the medial frontal/anterior cingulate cortex and bilateral insula on

unmodulated (but not on modulated) VBM analysis, failure of de-activation in the medial frontal/anterior cingulate cortex during performance of the *n*-back task, and decreased resting-state connectivity in the bilateral insula.

Conclusions

The findings provide evidence of brain abnormality in the medial frontal/anterior cingulate cortex and insula in delusional disorder. A role for the former region in the pathogenesis of delusions is consistent with several other lines of evidence.

Declaration of interest

None.

Copyright and usage

© The Royal College of Psychiatrists 2016.

Delusional disorder is a relatively uncommon disorder that is characterised by a single form of psychotic symptom. Patients develop a fixed abnormal belief that is often persecutory in nature, although it may take other forms, e.g. grandiose, hypochondriacal or of sexual infidelity.¹ Many but not all patients also experience delusions of reference. Other psychotic symptoms, in particular auditory hallucinations, are either absent or only minor and occasional. A minority of patients – 21% according to a recent study² – ultimately develop schizophrenia. Comorbidity with mood disorders, especially major depression, also seems increasingly likely;^{3,4} however, current diagnostic criteria require that the total duration of mood episodes is brief relative to the duration of the delusional periods.

As a disorder that shares clinical features with, and may sometimes progress to, schizophrenia, it would be of interest to know whether delusional disorder is associated with the kind of brain structural abnormalities seen in this and other psychiatric disorders. To date, however, only one structural imaging study has been carried out: Howard *et al*⁵ used magnetic resonance imaging (MRI) to measure brain and lateral ventricular volume in 19 patients with late-onset (>60 years) delusional disorder, 35 patients with late-onset schizophrenia and 35 healthy controls. The main finding was a significant increase in lateral ventricular volume in patients with delusional disorder compared with both the healthy controls and the patients with schizophrenia.

On the same grounds, it would be of interest to know whether delusional disorder is associated with brain functional changes. However, no functional imaging studies of the disorder using the kind of paradigms typically employed in schizophrenia – i.e. regional blood flow/metabolism at rest, functional magnetic resonance imaging (fMRI) during cognitive activation paradigms and recently functional connectivity analysis – have as yet been carried out. Some studies have investigated functional imaging

correlates of delusions, but these have been carried out in patients with schizophrenia⁶ or high-risk individuals⁷ and have been directed to test specific theoretical proposals, particularly Kapur's aberrant salience hypothesis.⁸

In this study, we report a combined structural and functional imaging study in a sample of well-diagnosed patients with delusional disorder. The principal aim was to establish whether and to what extent the disorder is associated with structural and functional imaging changes. We used voxel-based morphometry (VBM) to examine for presence of structural brain changes. Functional imaging (fMRI) was carried out during performance of a cognitive task, the *n*-back task, which has been extensively employed in schizophrenia and in several other psychiatric disorders. We also performed a resting-state functional connectivity analysis.

Method

Participants

The patient sample consisted of 22 individuals meeting DSM-IV⁹ criteria for delusional disorder. They were recruited via requests to clinicians working in hospitals, out-patient facilities and private practices in Barcelona and surrounding areas. Three patients were also recruited from an ongoing first-episode psychosis study in Barcelona; these were re-interviewed 2.5–4.5 years after illness onset and it was confirmed that none of them had undergone subsequent diagnostic shift. Clinical details on the patients are given in Table DS1 (online data supplement).

Diagnoses were established by means of a detailed clinical evaluation carried out by two of the authors (V.V. and P.J.M.). A structured psychiatric interview using the lifetime version of the Present State Examination (PSE), 9th edition,¹⁰ could be additionally performed in 19 of the patients (the remaining 3 either declined further examination after the initial interview or

*Joint last authors.

became unavailable). We also reviewed the patients' case records and spoke to clinicians who had been involved in their care. Patients were excluded if they were younger than 18 or older than 65, had past or present neurological disease/brain trauma, or had a history of alcohol/substance misuse prior to the onset of the delusional symptoms. In accordance with DSM-IV we included patients who had experienced depressive symptoms, as long as periods of these were short in comparison to the duration of the delusions (duration of depression is not operationally defined in DSM-IV, but all patients with more than minor depressive symptoms in our sample had experienced one or more periods of depression lasting weeks to months against a background of delusions that had been continually present for between 4 and 26 years; see Table DS1). We additionally required that patients did not meet criteria for major depression at the time of the study. Patients who had a history of mania were excluded.

Two of the patients were related to each other, but a diagnosis of shared psychotic disorder was excluded as the delusions had been present in both of them intermittently for several years, including while they lived separately, and the beliefs persisted when they were admitted to different hospitals.

The patients were all right-handed. Twenty were receiving treatment with antipsychotic drugs at the time of evaluation and scanning (atypical: $n=16$, typical: $n=4$), although adherence was doubtful in some. Six patients were also taking antidepressants. Two patients had never received treatment. All the patients were actively delusional at the time of evaluation.

The controls consisted of healthy adults individually matched 2:1 to the patients by age, gender and estimated premorbid IQ. They were recruited from non-medical staff working in the hospital, their relatives and acquaintances, plus independent sources in the community. They were questioned following a structured format and were excluded if they reported a history of mental illness, history of major mental illness in a first-degree relative and/or treatment with psychotropic medication apart from non-habitual use of anxiolytics/hypnotics. They were all right-handed.

Premorbid IQ was estimated using an IQ-validated version of the Word Accentuation Test (Test de Acentuación de Palabras, TAP);¹¹ this requires pronunciation of low-frequency Spanish words whose accents have been removed. The patients were also required to have a current IQ in the normal range (i.e. >70), as measured using four subtests of the Wechsler Adult Intelligence Scale III (WAIS-III)¹² (vocabulary, similarities, block design and matrix reasoning).

Written informed consent was obtained from all participants. The study was approved by the local research ethics committee.

Data acquisition

All participants were scanned in the same 1.5-T GE Signa scanner (General Electric Medical Systems, Milwaukee, Wisconsin, USA) at Sant Joan de Déu Hospital in Barcelona, Spain. During the scan the following sequences were obtained: (a) structural T_1 MRI; (b) fMRI during performance of the n -back task; and (c) resting-state fMRI.

Structural imaging

High-resolution structural T_1 MRI data were obtained with the following parameters: number of axial slices 180; slice thickness 1 mm, slice gap 0 mm, matrix size 512×512 ; voxel resolution $0.5 \times 0.5 \times 1 \text{ mm}^3$; echo time (TE) 4 ms, repetition time (TR) 2000 ms, flip angle 15° . Raw intracranial and global grey matter volumes were estimated with FMRIB Software Library (FSL)

SIENAX,¹³ which removes the non-brain matter and segments into grey matter and other tissues. VBM analyses were also conducted with FSL, with the exception of the normalisation step (see below) which was conducted with the 'advanced normalisation tools' (ANTS)¹⁴ due to their increased accuracy.¹⁵ VBM pre-processing included the following steps: (a) removal of non-brain matter; (b) segmentation into grey matter and other tissues; (c) affine registration of the native-space grey matter images to a Montreal Neurological Institute (MNI) template (voxel size: $1.5 \times 1.5 \times 1.5 \text{ mm}^3$); (d) creation of a template by averaging the affine-registered grey matter images; (e) non-linear registration of the native-space grey matter images to the template with the high-resolution symmetric normalisation (SyN) algorithm included in ANTS; (f) creation of another template; (g) three extra iterations of the steps (e) and (f); (h) non-linear registration of the native-space grey matter images to the last template; (i) modulation (based on the non-linear normalisation but not on the previous affine registration), and (j) $\sigma=3 \text{ mm}$ (equivalent to full width at half maximum (FWHM) 8 mm) Gaussian-smoothing (i.e. the kernel size recommended in VBM for its increased sensitivity¹⁶).

Differences between patients and controls were tested with threshold-free cluster enhancement (TFCE) statistics,¹⁷ thresholding the results at $P < 0.01$ family-wise error (FWE)-corrected for multiple comparisons, and findings were broken up using the seed-based d mapping 'imgcalc' tool (www.sdmproject.com/sdmtools/imgcalc/).¹⁸ TFCE replaces the t -value of each voxel by a value that also includes the amount of cluster-like local spatial support, thus making the statistical procedure a compromise between voxel- and cluster-based statistics. We compared images using both unmodulated and modulated VBM, since the former has been argued to have greater statistical power for detecting changes at the so-called mesoscopic level, i.e. between macroscopic and microscopic.¹⁶

Cognitive task fMRI

Participants performed a sequential-letter version of the n -back task¹⁹ in the scanner. Two levels of memory load (1-back and 2-back) were presented in a blocked design manner. The task included eight 48 s blocks (four 1-back and four 2-back blocks presented in an interleaved way), plus eight 16 s baseline stimuli presented between the blocks, thus having a total length of 8.5 min ($8 \times 48 \text{ s} + 8 \times 16 \text{ s} = 512 \text{ s}$). During the blocks, a single letter was projected in a screen (viewable by the participant through a mirror inside the scanner) every 2 s (1 s on, 1 s off), making a total of 24 letters per block. Five of these 24 letters were repetitions located at random; the participants had to respond to these by pressing a button. Characters were shown in green in 1-back blocks and in red in the 2-back blocks. The baseline

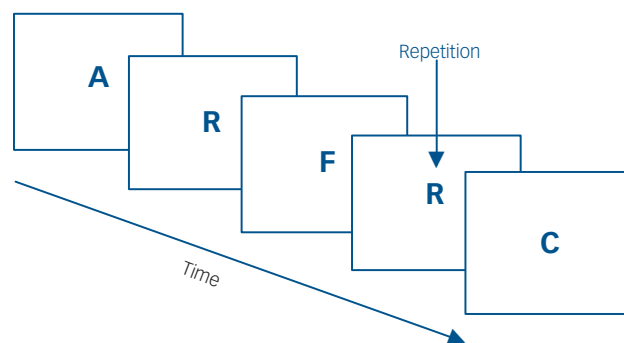


Fig. 1 Schematic of the n -back task.

stimulus was an asterisk flashing presented with the same frequency as the letters. The task is indicated schematically in Fig. 1.

All participants first went through a training session outside the scanner. Participants' performance was measured using the signal detection theory index of sensitivity, d' ,²⁰ which separately analyses true and false positives. Participants with negative d' values in either of or both of the 1-back and 2-back versions of the task, which suggests that they were not performing it, were excluded from this analysis.

During the task, a gradient-echo echo-planar (EPI) sequence depicting the blood oxygenation level-dependent (BOLD) contrast was acquired with the following parameters: number of volumes 266 (although the first 10 were discarded to avoid T_1 saturation effects), number of axial slices 16, slice thickness 7 mm, slice gap 0.7 mm, matrix size 64×64 , voxel resolution $3.1 \times 3.1 \times 7.7 \text{ mm}^3$, TE 20 ms, TR 2000 ms, flip angle 70° .

Pre-processing with FSL-FEAT included: (a) motion correction; (b) removal of non-brain matter; (c) $\sigma = 2 \text{ mm}$ (equivalent to FWHM 5 mm) Gaussian-smoothing (i.e. the default kernel size in FSL-FEAT); (d) grand-mean intensity normalisation of the entire 4D; (e) high-pass temporal filtering; (f) time-series statistical analysis with local autocorrelation correction; and (g) registration to a $2 \times 2 \times 2 \text{ mm}^3$ MNI template. To minimise unwanted movement-related effects, scans with an estimated maximum absolute movement $> 3.0 \text{ mm}$ or an average absolute movement $> 0.3 \text{ mm}$ were excluded from this analysis. The effects of stimulus-correlated motion were controlled by including the motion parameters in the model.

Differences in fMRI activation maps between patients and controls were analysed with FSL-FLAME stage 1 with default height threshold ($z > 2.3$).²¹ Again, the statistical maps were cluster-thresholded to $P < 0.01$ FWE-corrected for multiple comparisons and findings were broken down using SDM 'imgcalc' tool.

Resting-state connectivity

A resting-state fMRI sequence lasting 8 min 50 s was acquired with the same parameters used for the cognitive task. The computer screen was switched off and the individuals were instructed to lie quietly in the scanner with their eyes open to minimise the risk of falling asleep during the acquisition.

Prior to performing the connectivity analysis, several pre-processing steps were carried out, mainly using functions of the FSL package: (a) removal of non-brain matter; (b) motion correction; (c) regression by independent components with clear edge effects extracted by individual independent component

analysis (*melodic* function) to minimise residual movement effects; (d) registration to a $2 \times 2 \times 2 \text{ mm}^3$ MNI template; (e) $\sigma = 3 \text{ mm}$ Gaussian-smoothing (i.e. the kernel size used in previous analyses); and (f) regression by time-series from regions of interest (ROIs) located in cerebrospinal fluid and white matter to regress out global spurious trends. Once again scans with maximum movement of $> 3.0 \text{ mm}$ or mean movement $> 0.3 \text{ mm}$ were excluded from this analysis.

The analysis of resting-state connectivity was based on an overall measure of connectivity similar to those proposed by Buckner *et al.*²² and Cole *et al.*²³ Specifically, for each individual we calculated the average correlation between a voxel and each of the remaining voxels in the grey matter, leading to a brain map of average correlations. To reduce the computational burden, images were resampled to a voxel size of $4 \times 4 \times 4 \text{ mm}^3$. Temporal filtering (Butterworth filter) on low frequencies (0.02–0.1 Hz) was applied as well, as most relevant patterns of resting-state connectivity have been previously described in this low-frequency range.

Differences between connectivity maps of patients and controls were tested for using TFCE statistics,¹⁷ thresholding the results at $P < 0.01$ FWE-corrected for multiple comparisons, and a breakdown of the findings was made using the SDM 'imgcalc' tool again. The average amount of movement was included as a covariate to minimise any possible residual effect of movement not eliminated in the pre-processing steps.

Results

Demographic and clinical findings for the patients and controls are shown in Table 1. The two groups were well-matched for age, gender and estimated premorbid IQ (clinical information on the patients is in Table DS1).

Structural imaging

All patients and controls were included in this analysis. The patients had marginally lower mean intracranial and overall grey matter volumes, but the differences did not reach statistical significance (intracranial volume: $1\,076\,590$ v. $1\,084\,373 \text{ mm}^3$, reduction 0.7%, $t = 0.27$, $P = 0.8$; grey matter volume: $560\,063$ v. $568\,926 \text{ mm}^3$, reduction 1.6%, $t = 0.68$, $P = 0.5$).

Analysis of unmodulated images revealed reductions of cortical grey matter in the medial frontal/anterior cingulate cortex and bilateral insula/middle temporal gyrus; there were also reductions in sparsely distributed small clusters (Table 2 and Fig. 2(a)).

Table 1 Demographic and clinical characteristics of the samples

	Delusional disorder ($n = 22$)	Healthy controls ($n = 44$)	Comparison	P
Gender, male/female	10/12	20/24	$\chi^2 = 0$	1.00
Age, years; mean (s.d.)	45.1 (11.3)	45.2 (12.2)	$t = 0.03$	0.98
Estimated premorbid IQ; mean (s.d.) ^a	96.6 (11.0)	99.6 (10.5)	$t = 1.07$	0.29
Age at onset, years; mean (s.d.) ^b	36.7 (10.9)			
Duration of illness, years; mean (s.d.) ^b	8.4 (6.4)			
Type of belief				
Persecutory	17			
Erotomanic	1			
Hypochondriacal	1			
Mixed	3			

a. Information not available for one patient.
b. Information not available for four patients.
Further clinical details on the patients are in online Table DS1.

Table 2 Tabular description of the brain imaging findings^a

	Peak MNI	Size (voxels)	<i>P</i>	Cluster breakdown
Voxel-based morphometry (decreased volume)				
Medial frontal/anterior cingulate cortex and bilateral insula/middle temporal gyrus (BA 11 and 21 respectively)	60, -12, -12	3596	<0.001	Right middle frontal gyrus (946) Right inferior frontal gyrus (590) Right superior temporal gyrus (524) Right insula (485) Right rolandic operculum (354) Right precentral gyrus (177) Right Heschl gyrus (147) Right supramarginal gyrus (145) Right dorsolateral frontal cortex (80) Right postcentral gyrus (18) Right angular gyrus (19)
	-24, 30, -20	2965	0.001	Left inferior frontal gyrus (439) Left insula (423) Right medial/orbital frontal cortex (306) Left superior temporal gyrus (283) Left rolandic operculum (265) Left anterior cingulate gyrus (210) Left medial/orbital frontal cortex (182) Right anterior cingulate gyrus (151) Left middle frontal gyrus (117) Right gyrus rectus (100) Left Heschl gyrus (66) Left postcentral gyrus (59) Left precentral gyrus (54) Left gyrus rectus (48) Left supramarginal gyrus (39) Left middle temporal gyrus (48)
	-24, 54, 0	115	0.005	Left medial/orbital frontal cortex (37) Left middle frontal gyrus (27) Left dorsolateral frontal cortex (20)
	-54, -4, 48	113	0.007	Left postcentral gyrus (98) Left precentral gyrus (14)
	30, 38, -10	102	0.003	Right inferior frontal gyrus (52) Right middle frontal gyrus (48)
	-48, -72, 26	94	0.007	Left middle occipital gyrus (73) Left angular gyrus (12)
	54, 8, -36	86	0.004	Right inferior temporal gyrus (45) Right middle temporal gyrus (27)
	54, -56, 38	81	0.006	Left angular gyrus (38) Left inferior parietal gyri (35)
	-60, -54, 12	72	0.007	Left middle temporal gyrus (67)
	-54, 26, 22	53	0.004	Left inferior frontal gyrus (51)
	24, 60, -10	52	0.006	Right middle frontal gyrus (30) Right medial/orbital frontal cortex (21)
2-back task (failures of deactivation)				
Medial frontal/anterior cingulate cortex (BA 11)	4, 24, -8	1332	0.001	Medial/orbital frontal cortex (356) Anterior cingulate gyrus (242) Olfactory cortex (78) Gyrus rectus (30)
Resting-state (decreased connectivity)				
Bilateral insula (BA 48)	38, -10, 0	301	0.005	Right insula (110) Right putamen (56) Right rolandic operculum (14)
	-38, -16, -4	223	0.008	Left insula (78) Left rolandic operculum (37) Left supramarginal gyrus (26) Left Heschl gyrus (23)
MNI, Montreal Neurological Institute. a. Clusters with <50 voxels, regions with <10 voxels and white matter regions are not shown for simplicity.				

Analysis of modulated images did not yield significant differences between patients and controls. As noted in the Method, this could be a consequence of the fact that non-linear registration is able to capture gross, macroscopic variability such as brain shape abnormalities, but not more subtle mesoscopic differences such as cortical thinning. To test this hypothesis we applied surface-based morphometry of the structural data to ROIs

where there were unmodulated differences between the patients and the controls. This was done using the FreeSurfer software package (<http://surfer.nmr.mgh.harvard.edu>), which yields measures of thickness, area, mean curvature and volume in the chosen ROIs. The temporal VBM clusters were approximated by averaging the middle temporal, superior temporal and supra-marginal ROIs, and the mediofrontal VBM cluster by averaging

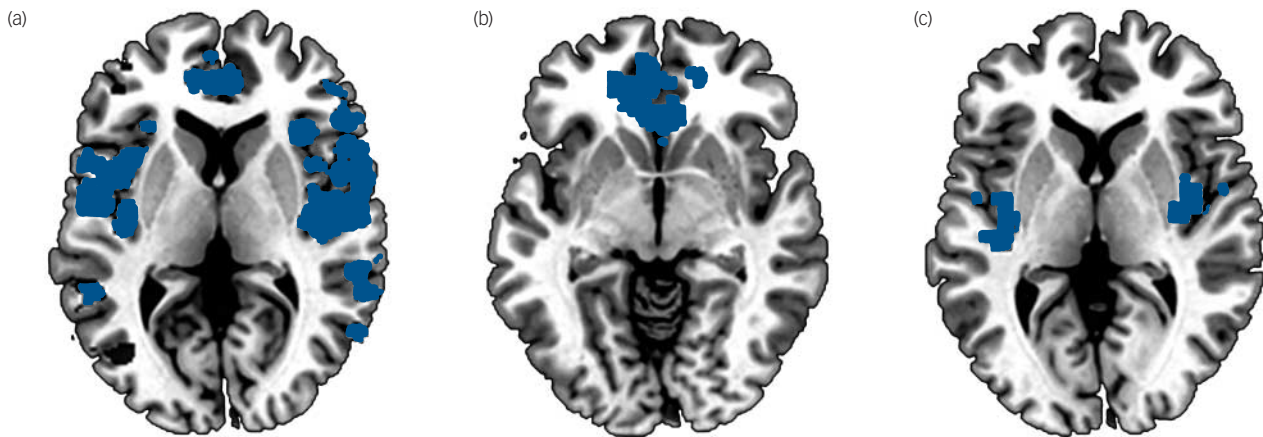


Fig. 2 Structural and functional imaging differences between the patients with delusional disorder and the controls. (a) Clusters of significant grey matter volume decrease in the anterior cingulate/medial frontal cortex and bilateral insula. (b) Cluster of significantly reduced de-activation in the 2-back *v.* baseline version contrast in the anterior cingulate/medial frontal cortex. (c) Clusters of significant decrease in resting-state connectivity in the bilateral insula.

the medial orbitofrontal, rostral anterior cingulate and superior frontal ROIs. The reduction of cortical thickness was found to be significant in most comparisons (right temporal reduction 3.9%, $P=0.002$; left temporal reduction 4.3%, $P<0.001$; right mediofrontal reduction 3.5%, $P=0.03$) but not in the left mediofrontal cluster (reduction 1.4%, $P=0.4$). No changes were observed in the other cortical measures with the exception of increased mean curvature in the right temporal cluster (increase 3.0%, $P=0.01$).

Both the unmodulated and modulated VBM findings were unchanged when the analysis was repeated excluding one of the two related patients.

Cognitive task fMRI

Four patients and six controls had to be excluded from this analysis due to excessive head movement. The remaining 18 patients and 38 controls continued to be matched for age (47.2 (s.d. = 11.6) *v.* 45.5 (s.d. = 12.0), $t=0.50$, $P=0.62$), gender (44.4% *v.* 47.4% males, $\chi^2=0.00$, $P=1.00$) and premorbid IQ (95.8 (s.d. = 11.3) *v.* 99.3 (s.d. = 11.2); $t=1.08$, $P=0.29$). No significant differences between the patients and controls were detected in stimulus-correlated motion ($P=0.12$), which was small or null in both groups. The patients performed significantly more poorly than the controls in both the 1-back ($d'=3.40$ (s.d. = 0.97) *v.* 4.30 (s.d. = 0.84), $t=3.28$, $P=0.003$) and the 2-back ($d'=2.26$ (s.d. = 1.07) *v.* 2.99 (s.d. = 1.09), $t=2.35$, $P=0.02$) versions of the task.

The 1-back *v.* baseline contrast did not reveal any significant differences in activation or deactivation between the two groups. However, in the 2-back *v.* baseline contrast, the patients showed a cluster of significant failure of deactivation in the medial frontal/anterior cingulate cortex (Table 2 and Fig. 2(b)). Extraction of mean cluster values confirmed that this was a region of deactivation in both groups; the mean BOLD response was -23.6 (s.d. = 19.3) in the controls and -7.2 (s.d. = 15.4) in the patients.

There was no correlation between the degree of medial frontal deactivation and performance (d'), either in the combined sample of patients and controls ($r=-0.08$, $P=0.56$) or when each group was considered separately (controls: $r=0.03$, $P=0.87$; patients: $r=0.09$, $P=0.71$).

Repeating the analyses after excluding one of the related patients or adding performance as a covariate resulted in no change to the findings.

Resting-state connectivity

Four patients and four controls had to be excluded from this analysis because of technical issues during acquisition, mainly head movement. The remaining 18 patients and 40 controls continued to be matched for age (46.5 (s.d. = 11.3) *v.* 45.3 (s.d. = 12.2); $t=0.37$, $P=0.71$), gender (44% *v.* 50% male, $\chi^2=0.016$, $P=0.91$) and premorbid IQ (96.1 (s.d. = 11.2) *v.* 99.5 (s.d. = 10.9), $t=1.08$, $P=0.28$).

Compared with the controls, the patients with delusional disorder showed a significant decrease in resting-state connectivity in the bilateral insula (Table 1 and Fig. 2(c)). Repeating the analyses after excluding one of the related patients did not affect the findings.

Discussion

This study found that patients with delusional disorder showed a pattern of structural and functional brain changes affecting the medial frontal/anterior cingulate cortex and the insula. Specifically, the patients showed reduced medial frontal/anterior cingulate grey matter volume reduction on unmodulated VBM and failure of de-activation in an overlapping area during working memory task performance. Additional volume reductions were found in the bilateral insula, and these were accompanied by lower resting-state functional connectivity in a similar region.

Structural changes in delusional disorder appear to share features with, but to be less widespread than, those seen in schizophrenia, the disorder with which it appears to have the strongest links in terms of shared clinical features and outcome. Thus, the medial frontal/anterior cingulate cortex and the insula are among the most consistently identified regions of cortical grey matter reduction in meta-analyses of MRI studies of schizophrenia.²⁴ In contrast, other notable regions of cortical volume reduction in schizophrenia, such as the dorsal and ventral lateral prefrontal cortex, were not seen in the patients with delusion disorder.

It should be noted that structural changes were only observed in our study when unmodulated VBM was used. This may reflect emerging evidence that subtle cortical volume changes – specifically those that are ‘mesoscopic’, i.e. between the macroscopic and microscopic level – are better detected by unmodulated VBM (e.g. see Radua *et al*¹⁶). This is a consequence of the fact that some changes are well-represented in the unmodulated images

whereas some are not well-captured by the non-linear registration, and so modulation only introduces macroscopic noise, ultimately reducing the statistical power. Such an interpretation was supported by further analysis of the regions of volume reduction identified by unmodulated VBM using surface-based morphometry; this found evidence of reduced cortical thickness, but not cortical area or volume reductions.

With respect to brain functional changes, cognitive task-related fMRI did not reveal statistically significant reduced activation in the dorsolateral prefrontal cortex or other regions of the prefrontal cortex in the patients. This is in contrast to schizophrenia, where the finding of task-related hypofrontality, although a somewhat inconsistent finding across individual studies, is supported by meta-analyses.^{25,26} On the other hand, we did find failure of de-activation in the medial frontal cortex, something that is now a well-replicated finding in schizophrenia²⁷ (see also Whitfield-Gabrieli *et al*²⁸ and Salgado-Pineda²⁹). Once again, therefore, delusional disorder appears to share some but seemingly not all of the functional imaging characteristics of schizophrenia.

Our finding of decreased resting-state functional connectivity in the bilateral insula, on the other hand, has less clear parallels with schizophrenia. Connectivity findings in this latter disorder are complex, with both increases and decreases having been documented, although the balance is in favour of decreased connectivity.³⁰ The subset of studies examining resting-state connectivity in schizophrenia have tended to implicate the medial frontal cortex as a major site of alteration,^{28,31,32} and changes in the insula have been reported, although less frequently.^{33,34}

In part, the heterogeneity of connectivity results in schizophrenia may be due to the intrinsic complexity of connectivity analyses. Compared with VBM or task-related fMRI where comparisons are essentially made for each voxel, connectivity analyses usually involve the relation between different sets of regions, and so the results will be highly dependent on the connections explored. Our approach based on maps of mean correlations, though, has a very wide scope and does not focus on specific connections or region sets. Voxels that emerge as significant in this analysis are simply those with mean correlation levels differing between the two groups and the analysis is not informative on the specific connections altered.

The question arises of whether our findings have implications for the pathogenesis of delusions. One currently influential theoretical approach to delusions is of dysfunction in a dopamine-mediated reward system.⁸ Regions that are important for reward processing include a subcortical structure, the ventral striatum, but also the medial frontal cortex which, together with the orbitofrontal cortex, is considered to be the principal cortical area where computation of the predictive value of rewards takes place (e.g. Haber & Knutson³⁵).

From another perspective, the medial frontal cortex is one of the major components of the so-called default mode network, a series of interconnected brain regions which are active at rest but de-activate during performance of a wide range of cognitive tasks.³⁶ According to Buckner *et al*,³⁶ there are two broad views of default mode network function. One is that it carries out a range of internally directed cognitive operations such as autobiographical recall, envisaging the future and theory of mind. The other is that it underlies a state of 'watchfulness', a passive, low-level monitoring of the external environment for unexpected events in conditions where active attention is relaxed. Both of these proposals have potential explanatory power for delusions, with the latter being particularly relevant to referential delusions. It is interesting to note in this context that Menon *et al*³⁷ recently found evidence for brain functional abnormality in the medial

frontal cortex, insula and ventral striatum in a study which compared patients with schizophrenia with prominent referential delusions and controls during performance of a task designed to elicit abnormal self-reference.

Much less is known about the function of the insula, a cortical region folded deep within the sulcus separating the temporal lobe from the frontoparietal lobes, which has extensive connections to many cortical and limbic areas, and appears to integrate cognitive, affective, sensory and autonomic information.³⁸ Palaniyappan *et al*³⁹ have argued on various grounds for a role for the insula in auditory hallucinations,⁴⁰ which commonly co-occur with delusions as part of the 'reality distortion' syndrome, and also for involvement in a specific form of delusions, passivity symptoms. However, the evidence they cite in support of this proposal has to be regarded as preliminary.

This study has some limitations. The sample size was relatively small, and so the possibility of both false positive and false negative findings cannot be discounted. Also, of necessity patients with different subtypes of delusional disorder were grouped together, and these might not be homogeneous in terms of underlying aetiology. Additionally, we did not explore the historical comorbidity with major depression seen in some of the patients, and other comorbidities were not investigated. Beyond this, we examined brain function using cognitive task activation, which might not be ideally suited to demonstrating hypoactivations in patients with delusional disorder, who are often presumed to be more cognitively intact than patients with schizophrenia (although the patients in our study showed impaired performance on the *n*-back task). It should also be noted that functional connectivity results are known to be affected by the type of motion correction used.⁴¹ We applied a strategy involving several different steps, but alternative approaches, such as the 'scrubbing' method recently proposed by Power *et al*⁴² might have given different results. Finally, it should be noted that most of the patients had taken and/or were taking antipsychotic drugs, which may itself have the capacity to produce changes in brain structure.

Victor Vicens, MD, FIDMAG Germanes Hospitalàries, CIBERSAM, Sant Boi de Llobregat, Spain, Benito Menni CASM, Barcelona, Spain and Psychiatry and Mental Health Program, Universitat de Barcelona, Barcelona, Spain; **Joaquim Radua**, MD, BStat, PhD, FIDMAG Germanes Hospitalàries, CIBERSAM, Sant Boi de Llobregat, Spain and Institute of Psychiatry, King's College London, London, UK; **Raymond Salvador**, BStat, PhD, **Maria Anguera-Camós**, BSc, **Erick J. Canales-Rodríguez**, BSc, **Salvador Sarró**, MD, FIDMAG Germanes Hospitalàries, CIBERSAM, Sant Boi de Llobregat, Spain; **Teresa Maristany**, MD, Hospital Sant Joan de Déu infantil, Barcelona, Spain; **Peter J. McKenna**, MD, **Edith Pomarol-Clotet**, MD, PhD, FIDMAG Germanes Hospitalàries, CIBERSAM, Sant Boi de Llobregat, Spain

Correspondence: Joaquim Radua, MD, PhD, FIDMAG Germanes Hospitalàries, C/Dr Antoni Pujadas 38-C, 08830 Sant Boi de Llobregat, Barcelona, Spain. Email: jradua@fidmag.com

First received 16 Oct 2014, final revision 20 Jan 2015, accepted 31 Jan 2015

Funding

This work was supported by the Centro de Investigación Biomédica en Red de Salud Mental (CIBERSAM) and several grants from the Instituto de Salud Carlos III-Subdirección General de Evaluación and the European Regional Development Fund (Rio Hortega contracts to VV (CM09/00297) and JR (CM11/00024), Miguel Servet Research contracts to RS (CP07/00048), EP-C (CP10/00596) and JR (CP14/00041); intensification grant to SS (10/231); project grants to RS (P10/01071), EP-C (P10/01058) and JR (P11/01766 and P14/00292) integrated into the National Plans 2008–2011 and 2013–2016 for research, development and innovation) and the Comisión per a Universitats i Recerca del DIUE from the Catalanian Government (2009SGR211).

References

- 1 Kendler KS. The nosologic validity of paranoia (simple delusional disorder). A review. *Arch Gen Psychiatry* 1980; **37**: 699–706.

- 2 Marneros A, Pillmann F, Wustmann T. Delusional disorders – are they simply paranoid schizophrenia? *Schizophr Bull* 2012; **38**: 561–8.
- 3 Maina G, Albert U, Bada A, Bogetto F. Occurrence and clinical correlates of psychiatric co-morbidity in delusional disorder. *Eur Psychiatry* 2001; **16**: 222–8.
- 4 de Portugal E, Martinez C, Gonzalez N, del Amo V, Haro JM, Cervilla JA. Clinical and cognitive correlates of psychiatric comorbidity in delusional disorder outpatients. *Aust N Z J Psychiatry* 2011; **45**: 416–25.
- 5 Howard RJ, Almeida O, Levy R, Graves P, Graves M. Quantitative magnetic resonance imaging volumetry distinguishes delusional disorder from late-onset schizophrenia. *Br J Psychiatry* 1994; **165**: 474–80.
- 6 Heinz A, Schlagenhauf F. Dopaminergic dysfunction in schizophrenia: salience attribution revisited. *Schizophr Bull* 2010; **36**: 472–85.
- 7 Juckel G, Friedel E, Koslowski M, Witthaus H, Ozgurdal S, Gudlowski Y, et al. Ventral striatal activation during reward processing in subjects with ultra-high risk for schizophrenia. *Neuropsychobiology* 2012; **66**: 50–6.
- 8 Kapur S. Psychosis as a state of aberrant salience: a framework linking biology, phenomenology, and pharmacology in schizophrenia. *Am J Psychiatry* 2003; **160**: 13–23.
- 9 American Psychiatric Association. *Diagnostic and Statistical Manual of Mental Disorders (4th edn, text revision) (DSM-IV-TR)*. APA, 2000.
- 10 McGuffin P, Katz R, Aldrich J. Past and present state examination: the assessment of 'lifetime ever' psychopathology. *Psychol Med* 1986; **16**: 461–5.
- 11 Gomar JJ, Ortiz-Gil J, McKenna PJ, Salvador R, Sans-Sansa B, Sarro S, et al. Validation of the Word Accentuation Test (TAP) as a means of estimating premorbid IQ in Spanish speakers. *Schizophr Res* 2011; **128**: 175–6.
- 12 Wechsler D. *Wechsler Adult Intelligence Scale (3rd edn) (WAIS-III)*. Psychological Corporation, 1997.
- 13 Smith SM, Zhang Y, Jenkinson M, Chen J, Matthews PM, Federico A, et al. Accurate, robust, and automated longitudinal and cross-sectional brain change analysis. *Neuroimage* 2002; **17**: 479–89.
- 14 Avants BB, Yushkevich P, Pluta J, Minkoff D, Korczynowski M, Detre J, et al. The optimal template effect in hippocampus studies of diseased populations. *Neuroimage* 2010; **49**: 2457–66.
- 15 Klein A, Andersson J, Ardekani BA, Ashburner J, Avants B, Chiang MC, et al. Evaluation of 14 nonlinear deformation algorithms applied to human brain MRI registration. *Neuroimage* 2009; **46**: 786–802.
- 16 Radua J, Canales-Rodriguez EJ, Pomarol-Clotet E, Salvador R. Validity of modulation and optimal settings for advanced voxel-based morphometry. *Neuroimage* 2014; **86**: 81–90.
- 17 Smith SM, Nichols TE. Threshold-free cluster enhancement: addressing problems of smoothing, threshold dependence and localisation in cluster inference. *Neuroimage* 2009; **44**: 83–98.
- 18 Radua J, Grau M, van den Heuvel OA, Thiebaut de Schotten M, Stein DJ, Canales-Rodriguez EJ, et al. Multimodal voxel-based meta-analysis of white matter abnormalities in obsessive-compulsive disorder. *Neuropsychopharmacology* 2014; **39**: 1547–57.
- 19 Gevins A, Cuttito B. Spatiotemporal dynamics of component processes in human working memory. *Electroencephalogr Clin Neurophysiol* 1993; **87**: 128–43.
- 20 Green DM, Swets JA. *Signal Detection Theory and Psychophysics*. Krieger, 1966.
- 21 Beckmann C, Jenkinson M, Smith SM. General multi-level linear modelling for group analysis in fMRI. *Neuroimage* 2003; **20**: 1052–63.
- 22 Buckner RL, Sepulcre J, Talukdar T, Krienen FM, Liu H, Hedden T, et al. Cortical hubs revealed by intrinsic functional connectivity: mapping, assessment of stability, and relation to Alzheimer's disease. *J Neurosci* 2009; **29**: 1860–73.
- 23 Cole MW, Pathak S, Schneider W. Identifying the brain's most globally connected regions. *Neuroimage* 2009; **49**: 3132–48.
- 24 Bora E, Fornito A, Radua J, Walterfang M, Seal M, Wood SJ, et al. Neuroanatomical abnormalities in schizophrenia: a multimodal voxelwise meta-analysis and meta-regression analysis. *Schizophr Res* 2011; **127**: 46–57.
- 25 Hill K, Mann L, Laws KR, Stephenson CM, Nimmo-Smith I, McKenna PJ. Hypofrontality in schizophrenia: a meta-analysis of functional imaging studies. *Acta Psychiatr Scand* 2004; **110**: 243–56.
- 26 Minzenberg MJ, Laird AR, Thelen S, Carter CS, Glahn DC. Meta-analysis of 41 functional neuroimaging studies of executive function in schizophrenia. *Arch Gen Psychiatry* 2009; **66**: 811–22.
- 27 Broyd SJ, Demanuele C, Debener S, Helps SK, James CJ, Sonuga-Barke EJ. Default-mode brain dysfunction in mental disorders: a systematic review. *Neurosci Biobehav Rev* 2009; **33**: 279–96.
- 28 Whitfield-Gabrieli S, Thermenos HW, Milanovic S, Tsuang MT, Faraone SV, McCarley RW, et al. Hyperactivity and hyperconnectivity of the default network in schizophrenia and in first-degree relatives of persons with schizophrenia. *Proc Natl Acad Sci USA* 2009; **106**: 1279–84.
- 29 Salgado-Pineda P, Fakra E, Delaveau P, McKenna PJ, Pomarol-Clotet E, Blin O. Correlated structural and functional brain abnormalities in the default mode network in schizophrenia patients. *Schizophr Res* 2011; **125**: 101–9.
- 30 Pettersson-Yeo W, Allen P, Benetti S, McGuire P, Mechelli A. Dysconnectivity in schizophrenia: where are we now? *Neurosci Biobehav Rev* 2011; **35**: 1110–24.
- 31 Salvador R, Sarro S, Gomar JJ, Ortiz-Gil J, Vila F, Capdevila A, et al. Overall brain connectivity maps show cortico-subcortical abnormalities in schizophrenia. *Hum Brain Mapping* 2010; **31**: 2003–14.
- 32 Ongur D, Lundy M, Greenhouse I, Shinn AK, Menon V, Cohen BM, et al. Default mode network abnormalities in bipolar disorder and schizophrenia. *Psychiatry Res* 2010; **183**: 59–68.
- 33 Liang M, Zhou Y, Jiang T, Liu Z, Tian L, Liu H, et al. Widespread functional disconnectivity in schizophrenia with resting-state functional magnetic resonance imaging. *Neuroreport* 2006; **17**: 209–13.
- 34 Moran LV, Tagamets MA, Sampath H, O'Donnell A, Stein EA, Kochunov P, et al. Disruption of anterior insula modulation of large-scale brain networks in schizophrenia. *Biol Psychiatry* 2013; **74**: 467–74.
- 35 Haber SN, Knutson B. The reward circuit: linking primate anatomy and human imaging. *Neuropsychopharmacology* 2010; **35**: 4–26.
- 36 Buckner RL, Andrews-Hanna JR, Schacter DL. The brain's default network: anatomy, function, and relevance to disease. *Ann N Y Acad Sci* 2008; **1124**: 1–38.
- 37 Menon M, Schmitz TW, Anderson AK, Graff A, Korostil M, Mamo D, et al. Exploring the neural correlates of delusions of reference. *Biol Psychiatry* 2011; **70**: 1127–33.
- 38 Critchley HD. Neural mechanisms of autonomic, affective, and cognitive integration. *J Comp Neurol* 2005; **493**: 154–66.
- 39 Palaniyappan L, Liddle PF. Does the salience network play a cardinal role in psychosis? An emerging hypothesis of insular dysfunction. *J Psychiatry Neurosci* 2012; **37**: 17–27.
- 40 Palaniyappan L, Balain V, Radua J, Liddle PF. Structural correlates of auditory hallucinations in schizophrenia: a meta-analysis. *Schizophr Res* 2012; **137**: 169–73.
- 41 Fair DA, Nigg JT, Iyer S, Bathula D, Mills KL, Dosenbach NU, et al. Distinct neural signatures detected for ADHD subtypes after controlling for micro-movements in resting state functional connectivity MRI data. *Front Syst Neurosci* 2012; **6**: 80.
- 42 Power JD, Barnes KA, Snyder AZ, Schlaggar BL, Petersen SE. Spurious but systematic correlations in functional connectivity MRI networks arise from subject motion. *Neuroimage* 2012; **59**: 2142–54.

